Transport properties through double-magnetic-barrier structures in graphene*

Wang Su-Xin(王素新)[a)b)], Li Zhi-Wen(李志文)[a)b)],
Liu Jian-Jun(刘建军)[c)], and Li Yu-Xian(李玉现)[c)†]

[a)] *Department of Physics, Hebei Normal College for Nationalities, Chengde* 067000, *China*
[b)] *Hebei Advanced Film Laboratory, Shijiazhuang* 050016, *China*
[c)] *College of Physics, Hebei Normal University, Shijiazhuang* 050016, *China*

(Received 7 December 2010; revised manuscript received 28 January 2011)

We study electrons tunneling through a double-magnetic-barrier structure on the surface of monolayer graphene. The transmission probability and the conductance are calculated by using the transfer matrix method. The results show that the normal incident transmission probability is blocked by the magnetic vector potential and the Klein tunneling region depends strongly on the direction of the incidence electron. The transmission probability and the conductance can be modulated by changing structural parameters of the barrier, such as width and height, offering a possibility to control electron beams on graphene.

Keywords: transmission probability, conductance, double-magnetic-barrier, graphene

PACS: 73.63.–b, 03.65.Pm, 75.70.Ak, 73.23.Ad **DOI:** 10.1088/1674-1056/20/7/077305

1. Introduction

Recently, graphene and graphene-based microstructures, which exhibit unusual properties and have potential technological applications especially as an alternative to the current Si-based technology,[1−3] have been realized experimentally.[4,5] Electronic confinement has been demonstrated in graphene microstructures using standard lithography methods,[6] which makes the fabrication of resonant-tunneling structures based on graphene practicable. Some studies have been devoted to tunneling through single- and multi-graphene barriers, wells, as well as several graphene-based junctions.[1,7−11] The charge carriers in these structures are described as massless and as chiral relativistic fermions governed by the Dirac equation. The Dirac-like quasi-electrons can result in unusual consequences in the electronic transport properties,[4,5], owing to their chiral characteristics. One peculiar phenomena is Klein tunneling,[12] which predicts that an electron can pass through high potential barriers with perfect transmission, in contrast to conventional nonrelativistic tunneling where the transmission probability exponentially decays with the increase of barrier height.[13−15] However, this feature is a weakness for the graphene to be fabricated into a heterostructure since Dirac electrons cannot be confined by electrostatic potentials. Many attempts have been made to overcome this shortcoming.[1−3]

Fortunately, several scholars have proposed an alternative way of confining the graphene electrons by magnetic field barriers or magnetic quantum dots.[16−18] The electronic properties in the presence of inhomogeneous perpendicular magnetic fields have attracted considerable theoretical attention.[19−25] On the basis of previous progress, we start the study of electron tunneling through a double-magnetic-barrier structure on the surface of monolayer graphene. The transmission probability and the conductance are calculated by using the transfer matrix method. The relationship between the transport properties of charge carriers and the parameters of double-magnetic-barrier structures will be discussed.

2. Model and formula

The system under consideration is an ideal double-magnetic-barrier structure on monolayer graphene. This model can be realized experimentally by depositing ferromagnetic strips on the top

*Project supported by the National Natural Science Foundation of China (Grant No. 10974043) and the Natural Science Foundation of Hebei Province of China (Grant No. A2009000240).

†Corresponding author. E-mail: yxli@mail.hebtu.edu.cn

© 2011 Chinese Physical Society and IOP Publishing Ltd

of a graphene layer. The height and the width of the left barrier are B_1 and d_1, and the height and the width of the right barrier are B_2 and d_2, respectively

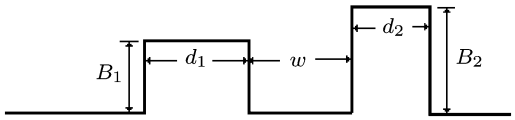


Fig. 1. Schematic representations of a double-magnetic-barrier structure.

(see Fig. 1). The barriers are separated by a nonmagnetic region of width w. Electrons in clean graphene close to the two Dirac points K and K' are described by two decoupled copies of the Dirac–Weyl (DW) equation. Here, we focus on a single valley and neglect the electron spin. Including the perpendicular magnetic field via minimal coupling, the DW equation reads

$$v_{\rm F}\boldsymbol{\sigma}\cdot\left(-\,{\rm i}\,\hbar\boldsymbol{\nabla}+\frac{e}{c}\boldsymbol{A}\right)=E\psi, \tag{1}$$

where $\boldsymbol{\sigma}=(\sigma_x,\sigma_y)$ is the Pauli matrix vector, and $v_{\rm F}\approx 0.86\times10^6$ m/s is the Fermi velocity in graphene. In the Landau gauge, $\boldsymbol{A}=(0,A(x),0)$, with $B_z=\partial_x A$. Thus, equation (1) is reduced to a one-dimensional form as

$$\begin{pmatrix} -E & -\,{\rm i}\,\partial_x-{\rm i}(k_y+A(x)) \\ -\,{\rm i}\,\partial_x+{\rm i}(k_y+A(x)) & -E \end{pmatrix}\psi=0. \tag{2}$$

The vector potential is given by

$$A(x)=\begin{cases} 0, & [-\infty,\ 0], \\ A_1, & [0,\ d_1], \\ 0, & [d_1,\ d_1+w], \\ A_2, & [d_1+w,\ d_1+w+d_2], \\ 0, & [d_1+w+d_2,\ +\infty]. \end{cases} \tag{3}$$

For convenience, we express all quantities in dimensionless units by means of two characteristic parameters, i.e., the magnetic length $l_B=\sqrt{\hbar/eB}$ and the energy $E_0=\hbar v_{\rm F}/l_{B_0}$. For a realistic value $B_0=0.1$ T, we have $l_{B_0}=811$ Å and $E_0=7.0$ meV, which set the typical length and energy scales.

Since the system is homogeneous along the y direction, the transverse wave vector k_y is conserved. The solution of Eq. (2) for a given incident energy E can be written as

$$\psi_{\rm w}=\,{\rm e}^{\,{\rm i}\,k_y y}\left[a_i\,{\rm e}^{\,{\rm i}\,k_x x}\begin{pmatrix}1\\ \dfrac{k_x+{\rm i}\,k_y}{E}\end{pmatrix}+b_i\,{\rm e}^{-\,{\rm i}\,k_x x}\begin{pmatrix}1\\ \dfrac{-k_x+{\rm i}\,k_y}{E}\end{pmatrix}\right] \tag{4}$$

in the well and

$$\psi_{\rm b}=\,{\rm e}^{\,{\rm i}\,k_y y}\left[c_i\,{\rm e}^{\,{\rm i}\,k_x x}\begin{pmatrix}1\\ \dfrac{k_x+{\rm i}\,q}{E}\end{pmatrix}+d_i\,{\rm e}^{-\,{\rm i}\,k_x x}\begin{pmatrix}1\\ \dfrac{-k_x+{\rm i}\,q}{E}\end{pmatrix}\right] \tag{5}$$

in the barrier. Here, $q=k_x+A$, and k_x is the longitudinal wave vector satisfying

$$k_x^2+(k_y+A_y)^2=E^2. \tag{6}$$

Using the continuity of the wave function at the boundaries, the transmission probability $T=|t|^2$ is then calculated by using the transfer matrix method.

According to the Landauer–Büttiker formula,[26] the ballistic conductance is calculated with the transmission probability as

$$G/G_0=\int_{-\pi/2}^{\pi/2}T(E_{\rm F},E_{\rm F}\sin\theta)\cos\theta\,{\rm d}\theta, \tag{7}$$

where θ is the incidence angle relative to the x direction and $E_{\rm F}$ is the Fermi energy. $G_0=2e^2E_{\rm F}L_y/(\pi h)$ is taken as the conductance unit, where $L_y\gg L$ is the width of the sample in the y direction.

3. Results and analysis

Firstly, we study the transmission probabilities each as a function of incidence angle for different structure parameters. The results are shown in Fig. 2. Figures 2(a) and 2(b) display the transmission probabilities for symmetrical double-magnetic-barrier structures with $d_1=d_2=w=1$ and $B_1=B_2$. From Figs. 2(a) and 2(b), we find that the transmission probability oscillates with the incidence angle and perfect transport appears at some oblique incidences instead of normal incidence. The shape of the transmission probability curve is asymmetric. Furthermore, the transmission probability is remarkable in a wide region of negative θ and is blocked by the barrier when the incidence angle exceeds a critical value. From Eq. (6), we know that evanescent states appear when the magnetic vector potential satisfies $|k_y+A_y|>|E|$. Thus the critical angle must be related to the Fermi energy and the magnetic field. From Figs. 2(a) and 2(b), we can see that the critical angle increases with the increase of Fermi energy and decreases with the

increase of the magnetic field intensity. Figures 2(c) and 2(d) are for the case of $B_1 = B_2 = 0.1$ T and $E_F = 5E_0$. It is clearly seen that the positions and the numbers of resonant peaks change with d_2 and w increasing, but the critical angle remains a common value. The angular dependence of the transmission probability is very remarkable. These features imply that both the width of the magnetic barriers and the width of the nonmagnetic region have effects on the angular dependence of the transmission probability but have no effects on the critical angle.

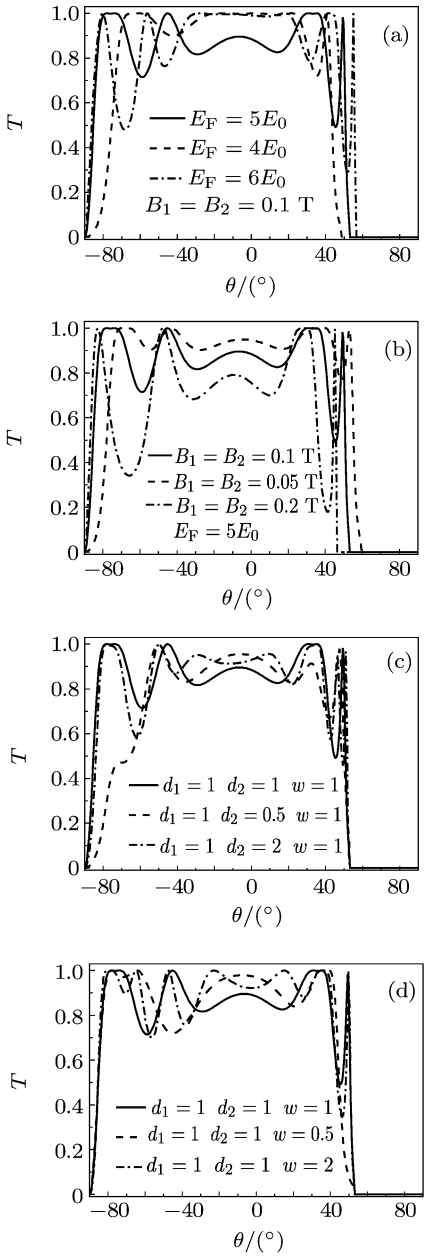


Fig. 2. Transmission probabilities each as a function of incidence angle with different structural parameters: (a) and (b) are for symmetrical double-magnetic-barrier structures with $d_1 = d_2 = w = 1$ and $B_1 = B_2$, and (c) and (d) are for asymmetrical double-magnetic-barrier structures with $B_1 = B_2 = 0.1$ T and $E_F = 5E_0$.

Figure 3 shows the energy dependence of the transmission probability for the double-magnetic-barrier with different structural parameters at normal incidence. Figures 3(a) and 3(b) are for a double-magnetic-barrier structure with $d_1 = d_2 = w = 1$. Figures 3(c) and 3(d) are for a symmetrical double-magnetic-barrier structure with $B_1 = B_2 = 0.1$ T. We can see that the transmission probability oscillates with the variation of Fermi energy at normal incidence. The resonant peaks are suppressed in the lower energy region. The shapes of the curves are closely

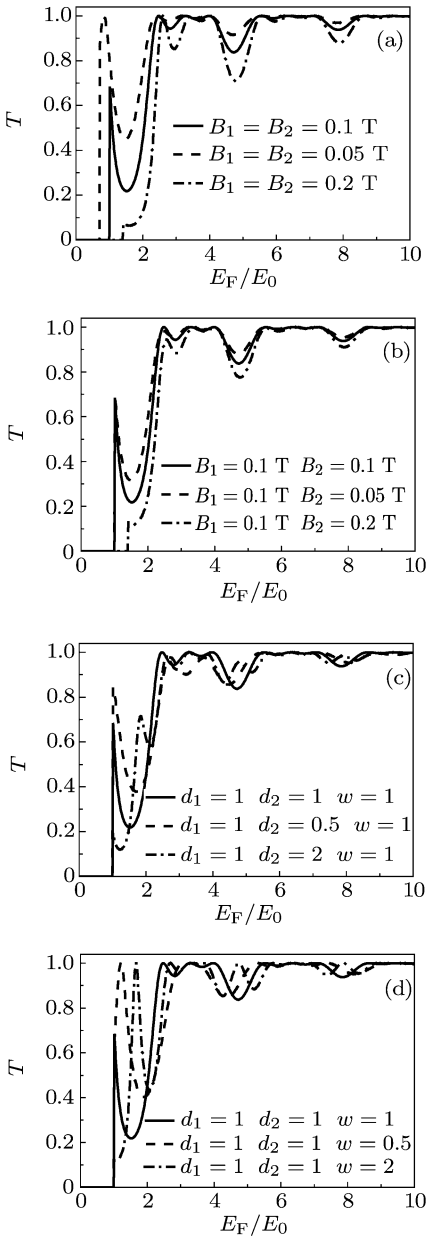


Fig. 3. Transmission probabilities each as a function of Fermi energy at normal incidence: (a) and (b) are for the structure with symmetrical barrier width at $d_1 = d_2 = w = 1$, and (c) and (d) are for the structure with symmetrical barrier height at $B_1 = B_2 = 0.1$ T.

related to the height and the width of the barrier. In other words, the normal incident transmission probability can be modulated by changing the structural parameters and the incident energy. It is well-known that perfect transport for normal incidence through pure electric-barrier structure in monolayer graphene is independent of the well width, the width and the height of the barriers. However, the situation is completely different for magnetic-barrier structures. These special properties offer the possibility to control electron beams on the graphene.

The properties of the transmission probability directly lead to the fact that angularly averaged conductance is related to the structural parameters. In Fig. 4, we plot the angularly averaged conductances each as a function of Fermi energy for the structure with symmetrical and asymmetrical barrier heights. The width of the magnetic barrier and the well are set to be the same and equal to 1 in units of l_B. There are a few interesting features exhibited in Fig. 4. The range of the conductance in each subplot changes from 0 to 1.85 in units of $2e^2E_{\rm F}L_y/(\pi h)$ and the conductance behaves like a wide shoulder for all cases. In Fig. 4(a), B_1 and B_2 are set to be the same. For this kind of symmetrical height magnetic barrier structure,

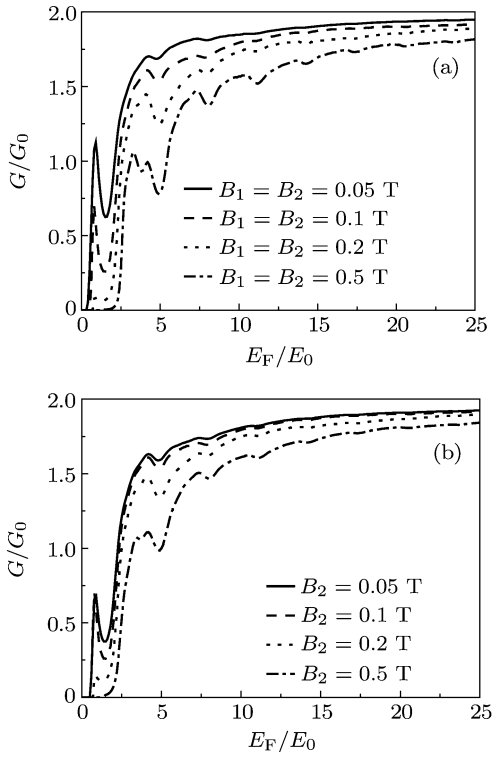


Fig. 4. Conductances each as a function of Fermi energy $E_{\rm F}$ for a double-magnetic-barrier structure with $d_1 = d_2 = w = 1$. (a) B_1 and B_2 are the same, (b) B_1 is fixed to be 0.1 T.

we can see that the conductance has a resonant peak in the lower Fermi energy region; with the increase of the magnetic intensity, the resonant peak and the step shift toward the right side are pressed together. Furthermore, Fig. 4(b) shows the angularly averaged conductances each as a function of Fermi energy for a magnetic structure with asymmetrical barrier height when the left magnetic field is set to be $B_1 = 0.1$ T. From Fig. 4, we can also observe that the conductance exhibits a drastic variation with the increase of barrier height at some suitable values of $E_{\rm F}$. For example, when the height of the barrier is changed from $B_1 = B_2 = 0.1$ T to $B_1 = B_2 = 0.5$ T at $E_{\rm F} = 0.5E_0$, the conductance decreases about 49%. In addition, when the height of the left barrier is fixed, the resonant peak is also suppressed by increasing the height of the right barrier. In Fig. 4(b), the conductance decreases about by 35% when the height of the right barrier is changed from $B_2 = 0.1$ T to $B_2 = 0.5$ T at $E_{\rm F} = 0.5E_0$.

To gain a deeper insight into the relationship between the conductance and the structural parameters, we present the conductances each as a function of B_2/B_1 in Fig. 5. The width of the structure is set to be $d_1 = d_2 = w = 1$, and the height of the left barrier is fixed to be $B_1 = 0.1$ T. From Fig. 5, we observe that the conductance is drastically reduced by increasing the height of the right barrier at a given Fermi energy. This is similar to the case of the transmission probability and can be understood in the same way.

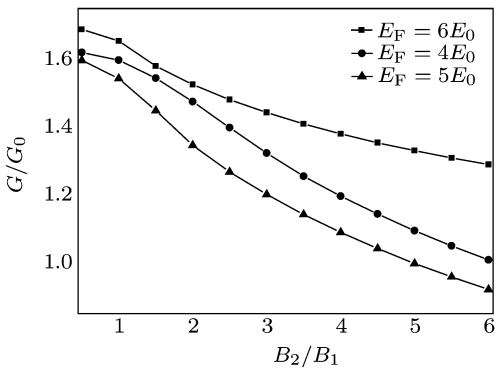


Fig. 5. Conductances each as a function of B_2/B_1 for a asymmetrical double-magnetic-barrier structure at different values of Fermi energy.

The thickness of the structure is an important parameter for designing devices based on the resonant tunneling effect. We find that the conductance depends sensitively on the width of the barriers. The conductances each as a function of d_1/d_2 for a double-magnetic-barrier structure with asymmetrical barrier

width are plotted in Fig. 6. It is shown that the conductance oscillates with d_2 increasing. The oscillation is drastic when the two barriers have the same width. In addition, the oscillation amplitude of the conductance decreases with the increase of the width of the right barrier. These results suggest an additional way of controlling the conductance of the present device.

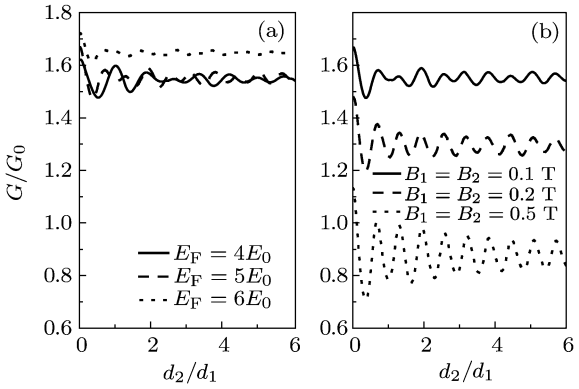


Fig. 6. Conductances each as a function of d_1/d_2 for a asymmetrical double-magnetic-barrier structure. The widths of the left barrier and the well are fixed to be $d_1 = w = 1$. (a) $B_1 = B_2 = 0.1$ T, (b) $E_F = 5E_0$.

4. Conclusions

Based on the transfer-matrix method, we investigate the transport properties of charge carriers through a double-magnetic-barrier structure on the surface of monolayer graphene. The transmission probability and the conductance through the structure are calculated and analysed. It is shown that the transport properties in the present structure are very different from those in an usual double-electrostatic-barrier. The transmission probability is blocked by the magnetic vector potential and the Klein tunneling region shifts towards the left side. The relationship between the transport properties and the structural parameters is also analysed in detail. The results indicate that the transmission probability and the conductance can be modulated by changing the heights or widths of the two barriers, thereby offering the possibility of practical applications in device design.

References

[1] Katsnelson M I, Novoselov K S and Geim A K 2006 *Nature Phys.* **2** 620

[2] Silvestrov P G and Efetov K B 2007 *Phys. Rev. Lett.* **98** 016802

[3] Cheianov V V and Falko V I 2006 *Phys. Rev.* B **74** 041403 disorder

[4] Novoselov K S, Geim A K, Morozov S V, Jiang D, Zhang Y, Dubonos S V, Grigorieva I V and Firsov A A 2004 *Science* **306** 666

[5] Zhang Y, Tan Y W, Stormer H L and Kim P 2005 *Nature* **438** 201

[6] Berger C, Song Z M, Li X B, *et al.*, 2006 *Science* **312** 1191

[7] Jin Z F, Tong G P and Jiang Y J 2009 *Acta Phys. Sin.* **58** 8537 (in Chinese)

[8] Bai C X and Zhang X D 2007 *Phys. Rev.* B **76** 075430

[9] Pereira Jr J M, Mlinar V and Peeters F M 2006 *Phys.Rev.* B **74** 045424

[10] Li Q, Cheng Z G, Li Z J, Wang Z H and Fang Y 2010 *Chin. Phys.* B **19** 097307

[11] Hu H, Cai J M, Zhang C D, Gao M, Pan Y, Du S X, Sun Q F, Niu Q, Xie X C and Gao H J 2010 *Chin. Phys.* B **19** 037202

[12] Klein O 1929 *Z. Phys.* **53** 157

[13] Li S S, Chang K and Xia J B 2006 *Phys. Rev.* B **68** 245306

[14] Li S S, Abliz A, Yang F H, Niu Z C, Feng S L and Xia J B 2002 *J. Appl. Phys.* **92** 6662

[15] Li S S, Abliz A, Yang F H, Niu Z C, Feng S L and Xia J B 2003 *J. Appl. Phys.* **94** 5402

[16] de Martino A, Dell'Anna L and Egger R 2007 *Phys. Rev. Lett.* **98** 066802

[17] Pan H Z, Xu M, Chen L, Sun Y Y and Wang Y L 2010 *Acta Phys. Sin.* **59** 6443 (in Chinese)

[18] Matulis A and Peeters F M 2007 *Phys. Rev.* B **75** 125429

[19] Park S and Sim H S 2008 *Phys. Rev.* B **77** 075433

[20] Oroszlany L, Rakyta P, Kormanyos A, Lambert C J and Cserti J 2008 *Phys. Rev.* B **77** 081403

[21] Zhai F and Chang K 2008 *Phys. Rev.* B **77** 113409

[22] Zhu R and Guo Y 2007 *Appl. Phys. Lett.* **91** 252113

[23] Li Y X 2010 *J. Phys: Condens. Matter* **22** 015302

[24] Büttiker M, Imry Y, Landauer R and Pinhas S 1985 *Phys. Rev.* B **31** 6207

[25] Xu H and Heinzel T 2008 *Phys. Rev.* B **77** 245401

[26] Buttiker M, Imry Y, Landauer R and Pinhas S 1985 *Phys. Rev.* B **31** 6207